DTP-96/47
February 1, 2008

Localized Solutions in a 2 Dimensional Landau-Lifshitz Model

B. Piette,
and
W.J. Zakrzewski
Department of Mathematical Sciences
University of Durham, Durham DH1 3LE, England
E-Mail: B.M.A.G.Piette@uk.ac.durham W.J.Zakrzewski@uk.ac.durham

ABSTRACT

We demonstrate the existence of stable time dependent solutions of the Landau-Lifshitz model with a constant external magnetic field. We find such solutions in all topological sectors, including N=0. We discuss some of their properties.

1. Introduction.

The dynamics of magnetic bubbles is an issue of practical interest [1]. A few years ago Papanicolaou and Tomaras [2] showed how to construct unambiguous conservation laws for systems described by the Landau-Lifshitz equation and pointed out the similarity of the gross features of the bubble dynamics to those of the familar Hall effect. This has stimulated more theoretical and numerical research. In particular in [3] an attempt was made to describe the dynamics of two bubbles. The model used in [3] was (2+1) dimensional and to stabilise the bubbles an additional "Skyrme-like" term was added to the more familar exchange, anisotropy and "magnostatic" terms. It was observed that the bubbles rotate around each other and that the dynamics of a system of one bubble and one antibubble exhibits the familar Hall motion.

The system in ref. [3] was modified in [4] to include an external magnetic field. This allowed the study of the so-called "golden rule" of bubble dynamics [5]. The introduction of the external magnetic field has suggested that we should have a serious look at the solution of the Landau Lifshitz equation with an (external) magnetic field. Hence in this paper we look at the case when this magnetic field is produced by the anisotropy of the system; thus we look at solutions of the Landau-Lifshitz equation for the anisotropic Heisenberg model here thought of as describing a magnetisation field.

So, the equation we want to study is

$$\partial_t \vec{\phi} = \vec{\phi} \wedge \left[\nabla^2 \vec{\phi} + A(\vec{\phi}.\vec{n})\vec{n}\right] \tag{1.1}$$

where $\phi = (\phi_1, \phi_2, \phi_3)$ is a unit vector describing the orientation of the magnetization, and $\vec{n} = (0, 0, 1)$ is the vector of the external magnetic field (or, put in other words, the

direction of anisotropy). We shall assume, in what follows, that the magnetization is defined over the two-dimensional plane $\vec{x} = (x, y)$.

There are two classes of interesting models describing such systems and they differ by the type of boundary condition that the magnetisation takes at infinity. There the field $\vec{\phi}$ can be required to be perpendicular to $\vec{n}$ (this defines the so called easy plane model) or we can require that it is parallel to $\vec{n}$ (this is the easy-axis model). In what follows we will be interested in the "easy-axis" model and, for this reason, we will consider the following expression for the total energy of the system

$$E = \frac{1}{8\pi} \int dxdy \Big[(\partial_x \vec{\phi}.\partial_x \vec{\phi}) + (\partial_y \vec{\phi}.\partial_y \vec{\phi}) + A(1 - \phi_3^2) \Big], \tag{1.2}$$

where A is a positive constant.

As one can be easily shown the time evolution (1.1) preserves the energy (1.2) . Another conserved quantity is given by the topological charge

$$Q = \frac{1}{4\pi} \int dxdy \Big[\vec{\phi}.(\partial_x \vec{\phi} \wedge \partial_y \vec{\phi}) \Big]. \tag{1.3}$$

The fact that the magnetization is required to take a single value at infinity means that the two dimensional plane can be thought of as being compactified to a sphere and the topological charge (1.3) which is normalised to take integer values, simply describes the number of times the field wraps itself around the sphere.

Instead of using the normalized vector $\vec{\phi}$ to describe the magnetization it is convenient to perform the stereographic projection of the sphere onto the complex plane and use the complex field

$$w = \frac{\phi_1 + i\phi_2}{1 + \phi_3}.$$

In this formulation the energy functional (1.2) takes the form

$$E = \frac{1}{2\pi} \int dxdy \Big[\frac{|w_x|^2 + |w_y|^2}{(1 + |w|^2)^2} + \frac{A|w|^2}{(1 + |w|^2)^2} \Big] \tag{1.4}$$

and the topological density is given by

$$Q = \frac{1}{2\pi} \int dxdy \Big[\frac{w_y^* \; w_x - w_x^* \; w_y}{(1 + |w|^2)^2} \Big]. \tag{1.5}$$

Finally, the equation of motion (1.1) becomes

$$iw_t + w_{xx} + w_{yy} - \frac{2w^*(w_x^2 + w_y^2)}{1 + |w|^2} - Aw\frac{1 - |w|^2}{1 + |w|^2} = 0. \tag{1.6}$$

When the external magnetic field is switched off, $A = 0$, and the static solutions of (1.6) are given by holomorphic functions of $z = x + iy$, namely, $w = w(x + iy)$.

2. Non Topological Periodic Solutions

In [6] a non static axially symmetric solution of the Landau-Lifshitz equation without an external field ($A = 0$) was presented and discussed. This solution was

shown to represent a wave-like field configuration whose energy density is in the form of rings propagating radially out towards infinity. When a term describing the interaction with a constant external magnetic field is added to (1.1) the situation is quite different. To see what happens in this case, we have, first of all, taken $w = 1/\sinh(r^2)$ as our initial condition and integrated (1.6) numerically.

We were very suprised to see that, at first, the ring expended a little and then settled down to a configuration periodic in time (after radiating out small rings of energy which propagated towards infinity).

A careful analysis of the final field as seen in our numerical simulation indicated that it was of the form

$$w = e^{-i\omega t} f(r), \tag{2.1}$$

where $f(r)$ is a real function. Inserting the ansatz (2.1) into (1.6) leads to the following equation for f

$$f_{rr} + \frac{f_r}{r} - \frac{2ff_r^2}{1+f^2} - Af\frac{(1-f^2)}{(1+f^2)} + \omega f = 0, \tag{2.2}$$

and the energy density (1.4) becomes

$$E = \int rdr\Big[\frac{f_r^2}{(1+f^2)^2} + \frac{Af^2}{(1+f^2)^2}\Big]. \tag{2.3}$$

However, the equation (2.2) is quite difficult to solve analytically but, on the other hand, it can easily be solved numerically using the shooting method or an over-relaxation technique. Before doing so, we notice that solutions of (2.2) minimize the functional

$$D = \int rdr\Big[\frac{f_r^2}{(1+f^2)^2} + \frac{Af^2}{(1+f^2)^2} - \frac{\omega f^2}{1+f^2}\Big]. \tag{2.4}$$

From this observation we note that, for any configuration f, performing the change of variable $r \to \lambda r$ leaves the first term in D unchanged but the last two terms get multiplied by λ^2. This means than unless the last two terms add up to zero we can always choose λ so that the energy of the configuration decreases under that transformation. This implies that for the non trivial solutions of (2.2) the last two terms in (2.4) must cancel out exactly:

$$\int rdr\frac{Af^2}{(1+f^2)^2} = \int rdr\frac{\omega f^2}{1+f^2}. \tag{2.5}$$

As for any non-vanishing f we have

$$\frac{f^2}{(1+f^2)^2} < \frac{f^2}{1+f^2}.$$

we can directly conclude that for any solution of (2.2) we must have

$$A > \omega.$$

To integrate (2.2) we start by analyzing the asymptotic behaviour of f. At infinity f must vanish to ensure that the total energy (1.4) is finite. At the origin, f must be of the form $f = K + Br^2 + O(r^3)$ where K is a constant depending on A and ω, and where $B = \frac{1}{4}\omega K + AK\frac{1-K^2}{1+K^2}$.

As we can always set A to 1 by redefining r as mentioned above, there is only one parameter in the equation which we choose to be ω. We have solved (2.2) using the shooting method for different values of ω in the range $0 < \omega < 1$ and have checked that (2.5) is satisfied for each solution. In Fig 1 we present the profiles for ϕ_3 as well as the energy density profiles for $\omega = 0.25, 0.5$ and 0.75. We note that when ω is small the energy density takes the form of a ring with a radius which gets larger as the value of ω decreases. We have also found numerically that the total energy of any solution is approximately given by the relation: $E = A/\omega$. We thus see that as the frequency increases the energy of the solution decreases while, at the same time, the solution becomes more localized. Note that all our solutions correspond to field configurations where ϕ_3 goes from a fixed value at the origin to the vacuum ($\phi_3 = 1$) at infinity. Moreover, the field precesses in the ϕ_1, ϕ_2 plane with the (constant) frequency ω.

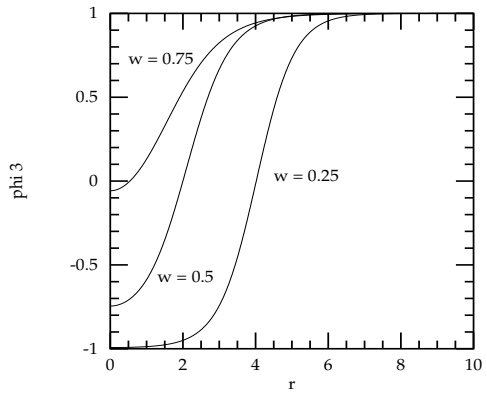

Figure 1.a : Non topological case. Profile of ϕ_3 for $\omega = 0.25$, 0.5 and 0.75

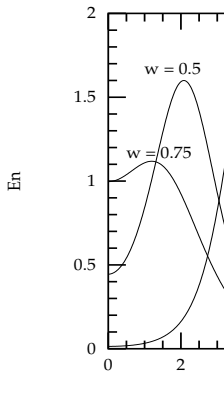

Figure 1.b : Non top
ergy profile for $\omega = 0$

It is clear from (2.1) and (1.5) that the topological density of the stationary solutions we have constructed is identically zero. These solutions are thus of a non topological nature.

To ensure that the solutions we have derived have solitonic properties we must verify that they are stable. Indeed, it could happen that a radially symmetric solution is an unstable configuration which desintegrates when it is slightly perturbed. To analyze this stability numerically we have decided to solve the full equation of motion

(1.6) numerically and we have also looked at the 1+1 dimensional PDE obtained by taking the ansatz $w = g(r,t)$, where g is a complex function:

$$ig_t + g_{rr} + \frac{g_r}{r} - \frac{2gg_r^2}{1+|g|^2} - Ag\frac{1-|g|^2}{1+|g|^2} = 0. \tag{2.6}$$

This ansatz is still radially symmetric but no specific time dependence is enforced. The reason for studying (2.6) is that the time evolution of its field progresses faster, and as a result, we are able to use finer grids and run our simulation for much longer lengths of equation time. Both sets of simulations have shown that, indeed, the solutions we have derived are stable. When perturbed, the ring "wobbles" around its position and emits small rings of energy which propagate out to infinity. By doing so, the ring loses some energy and eventually settles down to the original unperturbed stationary field configuration.

We have also subjected our solutions to several genuine 2d perturbations. These studies involved taking one of our configuration and adding to it one or two gaussian lumps centered at various points in x, y plane.

In particular we placed our nontopological structure at the origin and took $\omega = 0.5$. Thus, as can be seen from fig 1b, the energy density extends to $r \sim 5$. Then we added to w in (2.1) a gaussian perturbation of the form

$$w_{pert}(x,y) = A\, exp\Big(\frac{(x-a_0)^2 + (y-a_1)^2}{B}\Big), \tag{2.7}$$

and varied the values of parameters A, B, a_0 and a_1. All such perturbations gave qualitatively similar results. The perturbation deformed the field configuration which then evolved by sending out some energy and settling to a field configuration corresponding (2.1) to a value of ω which, in general, was different from the initial value. When the perturbation was not central *ie* if $a_0 \neq 0$ and $a_1 \neq 0$ then the resultant field configuration was deformed in a non-symmetric way and hence it moved in the direction opposite to the deformation (similar effects will be discussed in the next section).

We have also looked at the effect of two perturbations (both of type (2.7)) with the opposite values of a_0 and a_1. This time, as expected, the field evolved into a stationary configuration which, incidentally, corresponded to $\omega = 0.38$. The evolution was very rapid at first - the energy decreased from 3.6485 at $t = 0$ to 2.85 at $t = 40$ but then slowed down so that it reached 2.68 at t=615. All together our simulations have demonstrated the strong stability (and so indestructability) of our non-topological solutions. Moreover, in none of the simulations we have performed, have we seen the non-topological solutions being destroyed. The only exception to this (as we will describe later) is when two such configurations merge into one.

3. Moving Non topological Structures

The periodic configurations (2.1) satisfying (2.2) have also the remarkable property that they can be made to move at a constant speed if they are deformed in an

appropriate way. If we take as the initial condition for (1.6)

$$w = f(r)e^{i(ax+by)\pi}$$

where f satisfies (2.2) for a certain value of ω and where $k = (a^2 + b^2)^{1/2}$ is a constant then the field configuration describes an extended structure which moves at a constant speed in the direction of (a, b). The field still spins at the frequency ω but is slightly out of phase: the spinning at the front is retarded while that of the tail is advanced relative to the bulk of the structure.

The energy density of such a moving nontopological structure forms a ring which is virtually indistinguishable from that of the undeformed configuration (*i.e.* corresponding to $k = 0$). What is more interesting, is the topological charge density: though the total topological charge is zero, the topological charge density exhibits a peak and an anti-peak sitting side by side (Fig 2). The structure moves in the direction perpendicular to the line joining the peak and anti-peak, leaving the peak on its right-hand side.

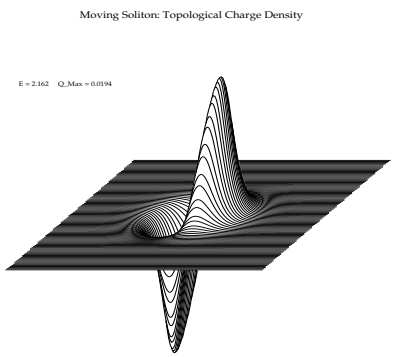

Figure 2 : Topological charge density of a moving structure. $(a, b) = (0, 0.1)$. En = 2.162, Qmax = 0.0194

In Table 1 we present the speed of translation for a few values of $k = (a^2 + b^2)^{1/2}$.

k	0.025	0.05	0.1	0.15	0.2
v	0.067	0.13	0.24	0.3	0.35
E	2.04	2.06	2.15	2.3	2.5

Table 1 : Speed of deformed structures, $\omega = 0.5$.

As we have moving structures we can study their scattering properties. To begin with we have scattered 2 structures with $\omega = 0.5$, initialy separated by 14 units. They have been made to move head-on using the initial condition

$$w_0 = f(r_1)e^{i\pi(y-b)k} + f(r_2)e^{-i\pi(y+b)k},$$

where $b = 7$, $r_1 = (x^2 + (y-b)^2)^{1/2}$, $r_2 = (x^2 + (y+b)^2)^{1/2}$ and $k = 0.1$. The two structures start by moving towards each other at a constant speed. Then they overlap and eventually perform a 90 degrees scattering. In Fig 3, we plot the energy density and the topological density of the initial configuration, and of the configuration after 40 units of time. We see clearly that each peak combines itself with the anti-peak of the other structure to form a new structure that emerges at 90 degrees.

Finally, it would be interesting to know how the non-topological structures interact when they are placed at rest next to each other. To answer this question, we have put two structures (both with $\omega = 0.5$) at rest so that they overlap a little. We took

$$w_0 = f(r_1) + f(r_2)$$

as our initial condition and have observed that the 2 structures initially moved towards each other. Then they scattered at 90 degrees without ever really escaping from each other. Then they moved backwards and scattered at 90 degrees again, radiating some energy. This cyclic motion was repeated many times, and at each step, the system lost a bit of energy. Eventually, the 2 structures merged into a single one which then was spinning at the frequency 0.37 and had an energy equal to 2.71.

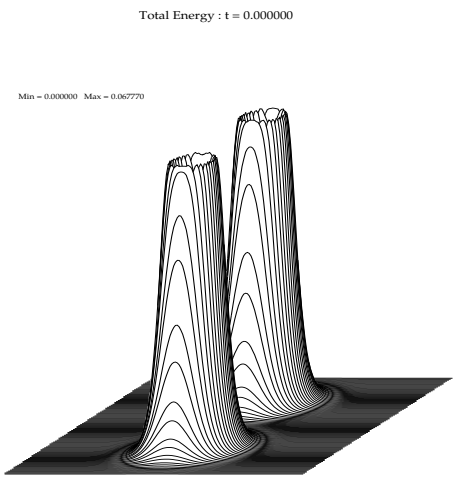

Figure 3.a : The periodic structure scattering, Energy density: t = 0

Figure 3.b : Topol
sity : t = 0

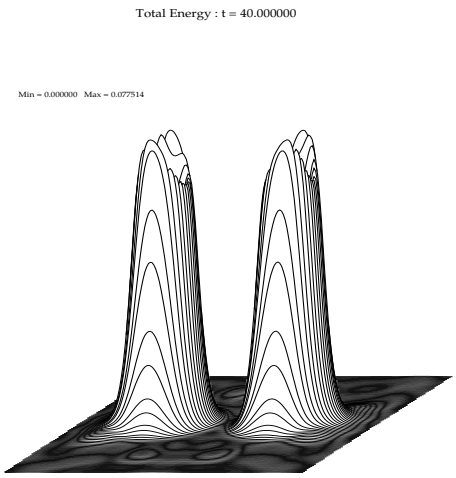

Figure 3.c : Energy density after the scattering : t = 40

Figure 3.d : Topol
sity : t = 40

We have also looked at the field configurations involving two structures corresponding to two different values of ω. To do this we placed at $x = 0$ $y = \pm 4$ the two nontopological field configurations corresponding to $\omega = 0.6$ (at $y = 4$) and $\omega = 0.5$ (at $y = -4$). Recall that as $E \sim A/\omega$ the field at $y = -4$ had higher energy. Like in the case mentioned before the two structures started spinning and attracted each other, performed a couple of oscillations at 90° and finaly evolved into a single structure spinning with $\omega \sim 0.42$. Most of the energy decrease took place during the initial oscillations (in fact by $t \sim 75$ the energy has already decreased from the initial value of 3.75 to 2.90); the single nontopological structure could be easily identified by $t \sim 50$ at which time it appeared at $x = 0$, $y \sim -1.8$ and then proceeded to move slowly towards more negative values of y. Hence the motion is dominated by the structure of higher energy and it proceeds in the direction towards its position. It is interesting to note that in both cases the resultant ω was lower than the initial ones.

This demonstrates that the non-topological nature of our periodic structures makes it possible for them to merge. As such, the number of structures is not conserved, but this is not surprising as the structures are nontopological and so their number is not expected to be conserved. On the other hand they are very stable as they don't decay or destroy themselves spontaneously.

4. Topological Periodic Solutions

In the previous sections we have seen that the easy axis model possesses non topological periodic solitons. Is it possible to find topological structures of a similar nature? We can, for example, take the ansatz

$$w = e^{-i\omega t} g(r) e^{in\theta} \tag{4.1}$$

where θ and r are the polar coordinates, n is an integer and $g(r)$ is a real function. The total topological charge (1.5) of such a configuration is n. Inserting the ansatz (4.1) into (1.6) leads to the following equation for g :

$$g_{rr} + \frac{g_r}{r} - \frac{2gg_r^2}{1+g^2} - \Big(A + \frac{n^2}{r^2}\Big)g\frac{1-g^2}{1+g^2} + \omega g = 0. \tag{4.2}$$

Before we proceed to solve this equation, let us notice that it can be derived by minimizing the functional

$$D = \int r dr \Big[\frac{g_r^2 + \frac{n^2 g^2}{r^2} + Ag^2}{(1+g^2)^2} - \frac{\omega g^2}{1+g^2}\Big]. \tag{4.3}$$

We then observe that the change of variable $r \to \lambda r$ leaves the first two terms in D unchanged but multiplies the last two by λ^2. This means that the last two terms must add up to zero, and again, we see that

$$A > \omega. \tag{4.4}$$

To integrate (4.2) we start by analyzing the asymptotic behavior of g. At infinity g must vanish to ensure that the total energy (1.4) is finite. At the origin, g must be of the form $g = r^n(K + Br^2 + O(r^3))$ where K is a constant depending on A and ω, and where $B = -K\frac{A+\omega}{4(1+n)}$. As for the non-topological configurations, we can always scale r to change the value of A. From now on we will thus set $A = 1$. (4.2) can then be integrated numerically and in Figure 4 we give the profile ϕ_3 and the energy density for different values of ω. Numerically, we find that for $n = 1$ the total energy is related to ω as : $E = -0.34 + 1.08/\omega$.

The first thing we must check is the stability of such solutions. To do this, we have solved (1.6) numerically using for the initial condition (4.1) where g satisfies (4.2) . We have found that even when we add a perturbation to the initial condition the solution is stable.

In Figure 4 we present the profile and the energy density of the topological configurations for different values of ω.

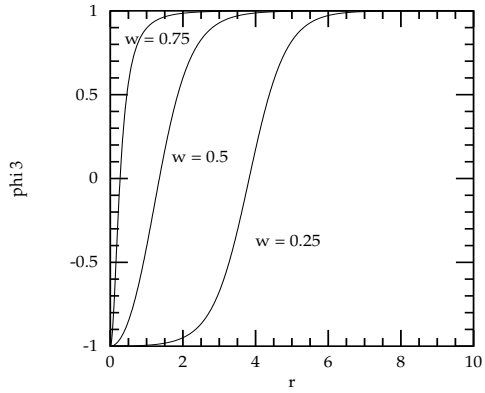

Figure 4.a : Topological structure ($n = 1$). ϕ_3 profile for $\omega = 0.25, 0.5$ and 0.75

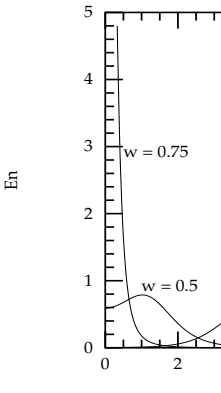

Figure 4.b : Energ
$0.25, 0.5$ and 0.75 ($\omega =$

Finally, let us emphasise the fact that for any value of N, (4.4) gives an upper bound for the largest value of ω for which a solution exists. We have tried to numerically determine the largest value of ω for with there is a solution. For $N = 0$ we have found solutions for values of omega very closed to 1. The largest value we have had success with was $\omega = 0.99$. For $N = 1$ we have found solutions for all values of ω up to $\omega = 0.95$. The most interesting case is $N = 2$: we found that $\omega < 5$. The largest successful value for which have found a solution was $\omega = 0.495$ with a total energy equal to 2.0005.

In Table 2 we give the total energy for some periodic solutions for $N = 0, 1$ and 2.

ω	0.1	0.2	0.3	0.4	0.5	0.6	0.7	0.8	0.9
$E(N=0)$	10	5.01	3.36	2.54	2.03	1.69	1.43	1.23	1.07
$E(N=1)$	10.03	4.97	3.28	2.38	1.82	1.44	1.19	1.13	1.0006
$E(N=2)$	7.81	3.76	2.73	2.30	-	-	-	-	-

Table 2 : Total energy of periodic solutions ($A = 1$)

5. Interaction between Topological Structures

Periodic topological structures are genuinely different from non-topological ones. The first evidence of this fact is obtained when two structures are placed next to

each other. For this we define $z_{\pm a} = x \pm a + iy$ and $r_{\pm a} = |z_{\pm a}|$, and use the following expression as an initial condition

$$w_0 = g_1(r_a)\frac{z_a}{r_a}e^{i\pi C} + g_2(r_{-a})\frac{z_{-a}}{r_{-a}}$$

where g_1 and g_2 both satisfy (4.2) with the angular velocity respectively equal to ω_1 and ω_2. The structures are centered around a and $-a$, and the term $e^{i\pi C}$ corresponds to the relative phase between them. We have performed various simulations for different values of C and have observed no qualitative difference.

We have taken different values for ω_1 and ω_2, namely: $(0.5, 0.5), (0.5, 0.4), (0.6, 0.4)$ and $(0.5, 0.45)$. When the two values of ω are different the behaviour is very similar: the configuration's field starts spining around the center of each structure and the structures begin to rotate along a circle (clockwise) centered at the mid point between them. At the same time, they interact with each other and, as a result, change their shape and their internal speed of rotation. The sizes of the two structures oscillate out of phase: as one them become spikier and spins faster the other one becomes broader and spins slower; then the situation is reversed. The first maxima are relatively high, but then the field configuration settles down to what looks like a periodic motion.

One could have expected that the two structures would progressively tune their angular rotation speed to eventually forming a configuration with both of them moving along a circle and spinning internally at the same speed. Our simulation shows that this is not the case: in each simulation the final configuration correponded to two stuctures moving along a circle and exchanging energy all the time. This exchange of energy makes them oscillate in size and modulates their internal spinning frequency.

This is partially confirmed by the simulation when the two ω have identical values. In this case, as expected, the fields start to spin with the angular frequency ω. At the same time the 2 structures start rotating around their midpoint. As the evolution progresses, the field configuration in the region between the two structures, initially of the form $\phi = (0, 0, 1)$, takes non trivial values in the ϕ_1, ϕ_2 plane ($\phi_3 = 0$). Apart from a regular rotation around the ϕ_3 axis the field is constant in this region. The energy density it generates is very small (virtualy invisible in the energy density graphs.) However, after a while, the region of constant ϕ starts to move between the 2 structures along a trajectory shaped like an "8" for which the structures are located in the middle of the two circles. This time, the size of the two structures oscillates in phase, but eventualy (at the fifth maximum in our simulation), as the energy is exchanged between the two structures, one of them becomes much larger than the other one and it spins internally much faster. As the structures becomes very spiky the number of lattice points supporting it becomes too small and the numerical simulation breaks down. It is difficult to decide, from a numerical point of view, if this blowup is a genuine effect or simply a numerical artefact, but we believe it is more likely to be a numerical problem rather than a genuine blow up. To resolve this problem we would have to take many more points for our lattice, something we are not able to do with the computers at hand.

Finally we have put 2 stuctures of different but very close angular frequencies $(0.5, 0.49)$ next to each other. The behaviour was very similar to what we saw when the frequencies were the same. Again, we are not able to determine whether this is a numerical problem or if the blow up is genuine.

Another interesting observation is the interaction between a structure and an anti-structure (*i.e.* a configuration with N = -1.) We can indeed put the two of them next to each other by using as the initial condition

$$w_0 = g(r_a)\frac{z_a}{r_a} - g(r_{-a})\frac{z^a_{-a}}{r_{-a}}.$$

In this case, the structure and the anti-structure move along approximately straight lines and the direction of motion is such that when looking forward, the structure is on the right-hand side. The lines are almost straight with an extra periodic oscillation imposed on them. In this they resemble the motion seen in [4] and [7].

We have performed different simulations for different values of ω and different value of the separation parameter a. We have found that the closer the structures are to each other, the faster they move. In Table 3, we give the speed observed in each of the simulation we have performed.

ω	0.4	0.4	0.5	0.5	0.6	0.6
a	0.2	0.3	0.2	0.3	0.2	0.3
v	0.18	0.14	0.21	0.12	0.11	0.018

Table 3 : The speed of Structure anti-Structure pairs.

We have also looked at the interaction when the structures had different angular frequencies. The main evolution was the same as before, the pair moved along approximately straight lines at a constant speed, but the deformation of the structures was more irregular and the oscillations of the structures along the lines where different.

6. Magnetic Bubbles

We mentioned in the introduction that the solutions of (1.6) when there is no magnetic field, $A = 0$, are given by holomorphic functions. The simplest solution is the so called magnetic bubble, which has a topological charge equal to 1 and is given by $w = \lambda(x + iy)$, where λ is a constant that fixes the size of the bubble. It would be interesting to know what happens when we take such a configuration as the initial condition when A is non-zero. This could be thought of as describing a system containing an isolated magnetic bubble which is suddenly immersed in a constant magnetic field.

Looking at (1.1) or (1.6) we notice that we have two parameters at hand, A and λ, but we can fix one of them by performing a rescaling of the coordinates. For our simulations, we have decided to keep λ constant and vary A; this way we can directly analyse how the strength of the magnetic field affects the magnetic bubbles. From now on we will thus assume that $\lambda = 1$.

What we have done, is to take the initial condition $w = x + iy$ and solve (1.1) for different values of A. When $A = 0$ the magnetic bubble is a static solution but as soon as there is a magnetic field the field starts to spin. In other words, the field takes the form of $w = g(r,t)e^{i(\theta+\omega t)}$ where r, θ are polar coordinates, $g(r,t)$ is a complex function (which varies with time) and ω is the angular speed of precession of the field. Notice that the initial condition is simply $t = 0$, $g(r) = r$. We have solved numerically both (1.1) and (4.2) and have found that the angular speed does not change with time. The main time evolution comes from the profile $g(r,t)$. The energy density shows that the bubble emits rings of energy which propagate towards infinity (we thus had to implement some absorption scheme to stop the wave from reflecting itself on the grid boundary). As the bubble radiates away some energy it progressively settles to a periodic configuration which is nothing but the solution described in section 4 with the corresponding value of ω. We have not found an argument to predict the value of ω (*i.e.* how ω depends on A.) In Table 4 we give some of the values we have observed in our simulations. When reading Table 4, one must remember that the solutions described in section 4 assume that $A = 1$. Thus the angular velocity listed in the table must be divided by the corresponding value of A before we can compare these solutions with those shown in Fig 4.

A	0.1	0.2	0.5	1	2	5
ω	0.072	0.13	0.278	0.48	0.82	1.47
E	1.15	1.30	1.59	1.90	2.33	3.35

Table 4 : Magnetic bubble energy and their angular velocity.

7. Conclusions

We have shown in this paper that the Landau-Lifshitz equation with an anisotropic term has various types of stable solutions periodic in time. All the solutions have the common property that the field spins internally at a constant speed. The solutions can have any topological charge or be topologicaly trivial. All the solutions are stable, in the sense that they can't be destroyed by small (and not so small) perturbations. The only exception are the non-topological solutions which can merge together to

form a new solution of the same type.

The non-topological structures have other surprising properties: they can be made to move at a constant speed by being deformed in a specific way. Such moving configurations scatter at 90 degrees.

The topological structures have different properties. When two of them are close to each other they move along a circle and exchange energy. Their size and internal angular speed of precession are periodic functions of time. Structures and anti-strcutures do not anihilate but move along essentially straight lines modulated by small oscillations.

Finally, when taken as an initial condition, holomorphic magnetic bubble modify themselves to become stationary solutions with internal field precession.

ACKNOWLEDGEMENTS

This work was initiated soon after we had some fruitful discussion with M. Lakshmanan and M. Daniel. We want to thank them both for sharing with us their knowledge of the Landau-Lifshitz model and for drawing our attention to ref [6].

We also wish to thank N. Papanicolaou and G. Stratopolos for helpful conversations.

References

1. see eg. A.P. Malozemoff and J.C. Slonczewski, Magnetic Domain Walls in Bubble Materials (Academic Press, New York) (1979)
2. N. Papanicolaou and T.N. Tomaras, *Nucl. Phys.* **B 360** 425 (1991), N. Papanicolaou, *Physica* **D 74** 107 (1994)
3. N. Papanicolaou and W.J. Zakrzewski, *Physica* **D 80** 225-245 (1995)
4. N. Papanicolaou and W.J. Zakrzewski, *Phys. Lett.* **A 210** 328-336 (1996)
5. T.H. O'Dell, Ferromagnetodynamics, the dynamics of magnetic bubbles, domains and domain walls (Wiley, New York) (1981)
6. M. Daniel, K. Porsezian and M. Lakshmanan - *J. Math. Phys.* **35** 12 (1994)
7. G.N. Stratopoulos and T.N. Tomaras - Vortex Pairs in charged fluids - Crete preprint 96-10 (hep-th/9601172)